

PITCH OSCILLATIONS OF A RECTANGULAR WING SECTION IN TRANSONIC FLOW

C. Hillenherms, W. Schröder, W. Limberg
Aerodynamisches Institut der RWTH Aachen
Wüllnerstraße zw. 5 und 7, D-52062 Aachen, Germany
Phone: +49-(0)241-809 55 71, Fax: +49-(0)241-809 22 57
e-mail: conny@aia.rwth-aachen.de

Keywords: *unsteady, transonic, pitch oscillation*

Nomenclature

a	Sonic speed
c	Airfoil chord
c_l	Lift coefficient
c_m	Moment coefficient (+ nose up)
$c_p = \frac{p-p_\infty}{q}$	Pressure coefficient
c_p^*	Critical pressure coefficient
F_α	Pitching frequency
$Ma = u_\infty/a$	Freestream Mach number
$q = \rho_\infty/2 u_\infty^2$	Dynamic pressure
$Re = \frac{u_\infty c}{\nu}$	Reynolds number
u_∞	Freestream velocity
α	Angle of attack (+ nose up)
$\bar{\alpha}$	Mean angle of attack
α_{static}	Static angle of attack
$\alpha(t)$	Pitching motion (+ nose up)
$\Delta\alpha$	Pitching amplitude
ρ_∞	Density, undisturbed fluid
$\omega_\alpha = 2\pi F_\alpha$	Angular pitching frequency
$\omega^* = \frac{c}{u_\infty} \omega_\alpha$	Reduced frequency

Abstract

The interaction of aerodynamic and structural forces on a 2-D rectangular wing section oscillating in pitch is studied at transonic flow. The investigations include self-sustained as well as forced

oscillations. The free pitching motion is generated by a symmetric elastic suspension on both sides of the rigid wing, whereas the forced oscillations are induced by an electric actuator on one side of the model. The investigations are based on the simultaneously measured aerodynamic forces and surface pressures while the wing section is in motion. The wing model is oscillating about mean incidence angles of zero to two degrees at Mach numbers of 0.50 up to 0.85, corresponding to Reynolds numbers 1.5 to 2.2 million. The wing has a supercritical BAC 3-11/RES/30/21 airfoil with a relative thickness of 11% [6]. Preliminary investigations include measurements of the steady pressure distribution and flow visualization at transonic Mach numbers for a fixed mounted wing model with the same airfoil.

1 Introduction

The prediction of stability boundaries is one of the most essential tasks in today's aircraft design process. As a consequence, efficient design tools have to be developed that are based on numerical simulations of the fluid-structure interaction. However, the development of reliable aeroelastic codes requires experimental data to assess the accuracy and validity of the computed results. Besides the validation of numerical methods, the experiments serve for the study of physical phenomena like shock/boundary-layer interaction.

2 Experimental setup

2.1 Decaying oscillations

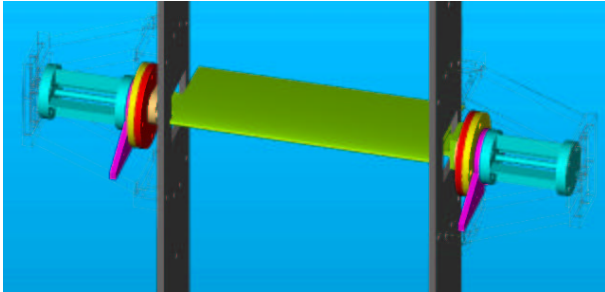


Fig. 1 Elastically mounted rectangular wing section

Figure 1) shows the model mounting for free pitching motion with an elastic suspension on both sides. The grey panels symbolise the side walls of the test section. The wing model is mounted to a two-component strain-gauge balance on each side of the test section. The balance gives the lift and drag components whereas the torsional moment is measured by means of two symmetrical torsional springs which also serve as an elastic mount and allow the wing to pitch. The torsion springs themselves are fixed to the wall-mounted support. The time-dependent angle of attack of the model is taken on one side of the test section by two laser triangulators pointing on the violet lever. A more detailed description of this setup can be found in Ref. [3].

2.2 Forced oscillations

For the generation of forced pitch oscillations the torsion springs are removed and replaced by pivoted shafts. On one side of the test section an excitation assembly is mounted (Fig. 2), consisting of a lever and an adjustable excenter which is driven by a 5.5 kW asynchronous motor and a frequency converter. It allows excitation frequencies up to 100 Hz. The pitching motion is again measured by two laser triangulators on the other side of the test section.

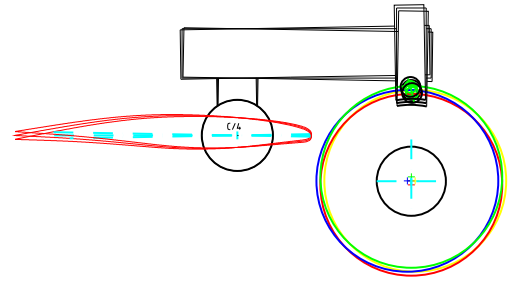


Fig. 2 Scheme of the wing section with electrical excitation

2.3 Wind tunnel

The investigations are carried out in the transonic wind tunnel of the Aerodynamisches Institut. The suction type wind tunnel operates intermittently at atmospheric pressure and temperature, and allows test periods of 2 to 5 seconds. Two test sections each of $0.4 \times 0.4 \text{ m}^2$ are available, either with fixed or with 2-D-adaptive walls. The test section with adaptive upper and lower walls allows interference-free measurements in transonic flow [7]. The flexible walls are made of spring steel plates clamped to 24 traversing stages with stepping motors (Fig. 3). The wall contours are calculated using the linearized theory for compressible flows and Cauchy's integral formula based on the measured wall pressure distribution and the wall contour [1].

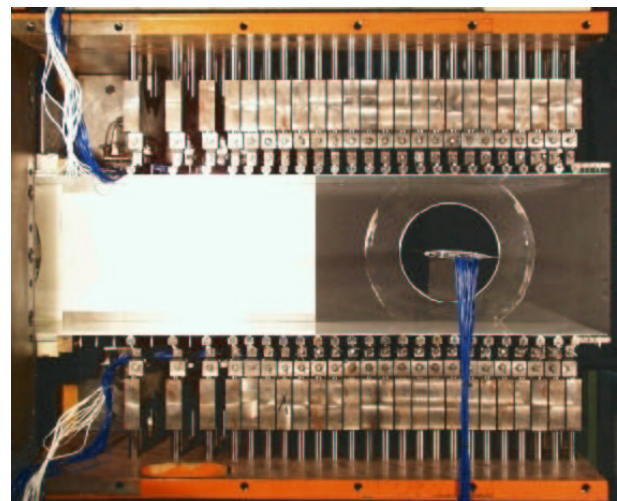


Fig. 3 Adaptive test section

Even for unsteady investigations, a steady adaptation of the walls reduces a large amount of

wall interference effects and only residual interferences have to be corrected [10]. For this purpose, each of the adaptive walls is equipped with 13 pressure sensors for the assessment of unsteady wall pressures.

2.4 Airfoil model

In the present investigation two models are applied for unsteady measurements, and a third one was used for steady testing that will not be described in the following. The first model for unsteady testing was used for the decaying oscillations whereas the second one was used for the forced oscillations. All models have a 150 mm chord and a 400 mm span. They are made of carbon fiber reinforced plastics to ensure minimum inertial forces and moments. The first one is equipped with eleven, the second one with thirty sub-miniature pressure sensors in the mid-span (Fig. 4). More details of the sensor mounting in that last model are given in the next section (2.5). Bending stiffness is obtained by glass fiber and aluminum spars, respectively, whereas the shells contribute the major part of the torsional stiffness of the model. Aluminum and steel flanges, respectively, on either side are necessary to transmit the forces and moments, and to bolt the model to the other devices.

2.5 Pressure measurement technique

The wind tunnel model is equipped with piezo-resistive pressure sensors to prevent damping and a low pass response of the unsteady pressure signals due to long tubing. The cylindrical sensors are mounted into a special aluminum rib inside the model (Fig. 4). The fixation and the sealing of the sensors is achieved by screwing them into the central rib together with O-rings, leaving only a very small cavity in front of the sensor head and a connection to the surface pressure taps of 0.3 mm diameter. Only the sensors at the leading edge and at the most aft position had to be connected to the surface pressure taps by longer tubes, because of the restricted space in the model.



Fig. 4 Upper shell of the second model with rib, spars and flanges

2.6 Force measurement technique

The unsteady forces are measured by a strain-gauge balance made out of maraging steel which is particularly suited for the construction of strain gauge balances due to its extremely high yield strength [5]. It consists of two pairs of circular panels mounted on both sides of the airfoil model in the case of free oscillations. In the case of forced oscillations only one pair is used on the excitation side since on the other side it would represent only an additional inertia. One panel of each pair is to measure the forces in the chordwise direction, whereas the other panel measures the forces perpendicular to the model chord. The panels have four bending beams equipped with strain-gauges to register the beam deformation caused by an acting force. On every beam the strain-gauges are assigned to a full Wheatstone bridge. The calibration has confirmed that the balance design provides minimum interference of the different stress modes and minimum sensitivity to torsion.

2.7 Data acquisition

The data is sampled simultaneously by a system of five data acquisition boards installed in a personal computer. The synchronized boards allow maximum sampling of 40 channels at 1.25 MHz with 12 bit resolution. The pressure signals are low-pass filtered and amplified by DC amplifiers,

whereas the strain-gauge signals are processed by a 5 kHz carrier frequency amplifier.

3 Results

3.1 Steady measurements

Measurements of the steady pressure distribution and flow visualisation of the fixed model have been made in the two different test sections and with free and forced transition, respectively. A comparison of these different flow cases is displayed in Figure 5 in terms of the lift coefficient with respect to the Mach number for different angles of attack. It can be stated that the Mach

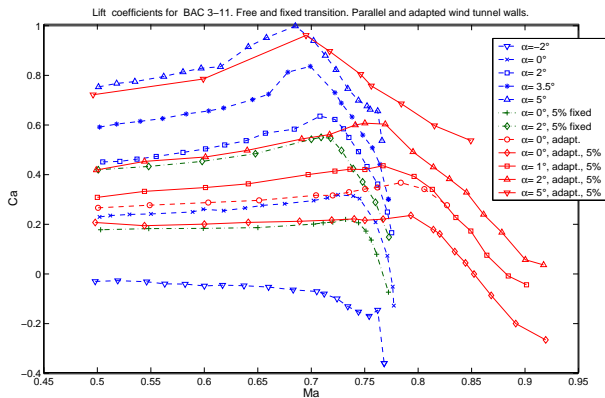


Fig. 5 Measured lift coefficients for transonic Mach numbers and different angles of attack, with free (blue) and forced transition at 5 % chord (green), with parallel and adapted walls (red)

number envelope is clearly enhanced by wall adaptation, and that the maximum lift coefficients and the corresponding Mach numbers are shifted towards higher values for all measured angles of attack save for 5° where the wall adaptation is not able to totally eliminate wall interference effects due to the expanded supersonic region on the upper side of the model.

Numerical Calculations with the Euler–boundary-layer method MSES [2] have been done in order to check the reliability of the wall adaptation. For this purpose, the farfield boundary condition was set to infinite-flow to simulate freeflight conditions. The comparison of the measured and calculated pressure distributions yields a very good agreement for nearly all flow

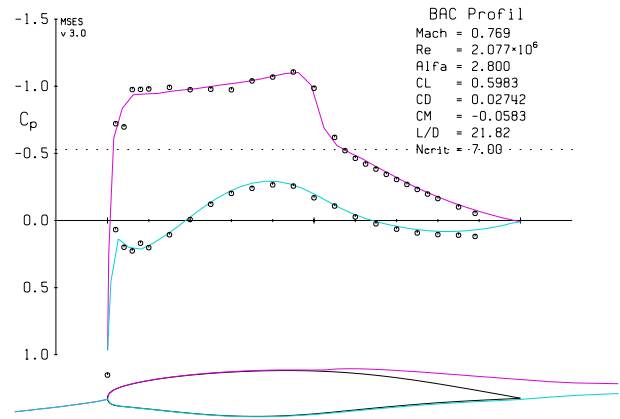


Fig. 6 Comparison of measured (symbols) and calculated (line) pressure distribution for $Ma = 0.77$, $Re = 2.077 \times 10^6$, and $\alpha = 2^\circ$

cases. An example is presented in Figure 6 for a Mach number of 0.77, and an angle of attack of $\alpha = 2^\circ$ with a pronounced supersonic area on the upper side of the airfoil and presumably a combined shock-induced/trailing edge separation. Of course the perturbation effect of the transition strips at 5% profile chord does not emerge as distinctive as in the experiment since the strip itself is not modeled.

3.2 Unsteady measurements

3.2.1 Decaying pitch oscillations

Decaying and self-sustained pitch oscillations have been carried out at Mach numbers of 0.50 to 0.85 and static angles of attack between 0° , 2° , and 2.5° [4]. The static angle of attack α_{static} is the angle of attack in still air. During the test run, the mean angle of attack adjusts on lower values because of the elastic suspension and the (mean) negative pitching moment. After an initial angular deflection, the model is released under steady flow conditions. The pressure distribution, the reactions, and the instantaneous angle of attack are measured simultaneously.

The pitching motion was decaying in all measured cases, i.e. the damping was always positive, and the system remained stable. Figure 7 shows the damping coefficients determined from the decaying part of the pitch oscillation which results in a relatively strong scattering of the values. The

different symbols indicate the variation of the static angle of attack. The damping coefficient is in-

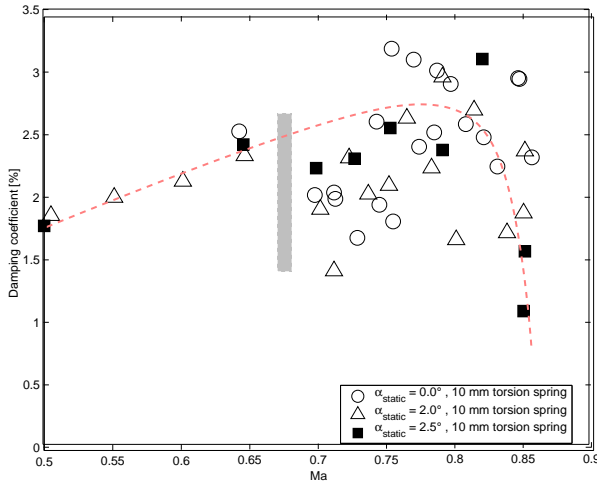


Fig. 7 Damping coefficient with respect to the Mach number

creasing for Mach numbers rising from 0.50 to 0.80. But it is steeply decreasing for higher Mach numbers. No reliable statement can be made if this gradient continues until the damping coefficient becomes negative for even higher Mach numbers, since the extent of the supersonic region and the strength of the existing shocks prohibit a reasonable wall adaptation.

A look at the steady measurements, more precisely at the pitching coefficient, leads to a possible interpretation of the trend of the damping distribution. As can be seen in Figure 8, the minimum moment coefficient coincides with the maximum lift coefficient (Fig. 5) at a Mach number of 0.76 for an angle of attack of 2°. The moment coefficient is rising sharply for higher Mach numbers and becomes positive at a Mach number of 0.86. This is similar for angles of attack of 1° and 0°, respectively, and underlines the assumption of a beginning torsional instability.

3.2.2 Forced pitch oscillations

At Mach numbers of 0.50 to 0.85 and mean angles of attack between -1° and 2°, forced pitch oscillations have been carried out with excitation frequencies of 45, 60, and 90 Hz and amplitudes of 0.2° and 0.4°. The reduced frequencies were thus ranging from 0.15 to 0.51. Again the pres-

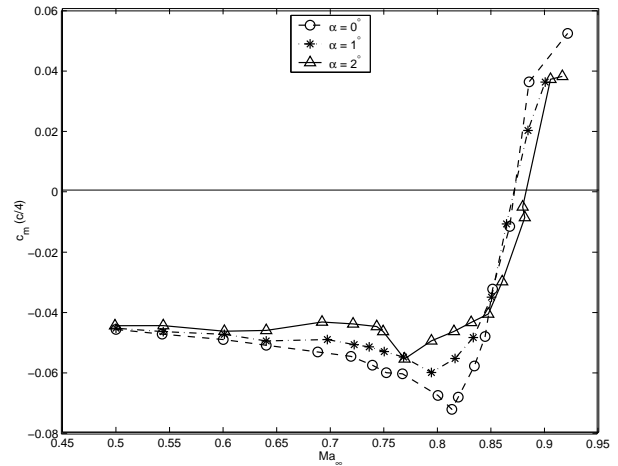


Fig. 8 Pitching moment coefficient depending on the Mach number for $\alpha = 0^\circ, 1^\circ,$ and 2° from steady pressure measurements

sure distribution, the reactions, and the pitching motion are measured simultaneously.

Pressure fluctuations on the upper side of the pitching airfoil are displayed in Figures 9 and 10 for different Mach numbers at a mean angle of attack of 1.5° and the two pitching amplitudes of 0.2° and 0.4°, respectively, in terms of root-mean-square values.

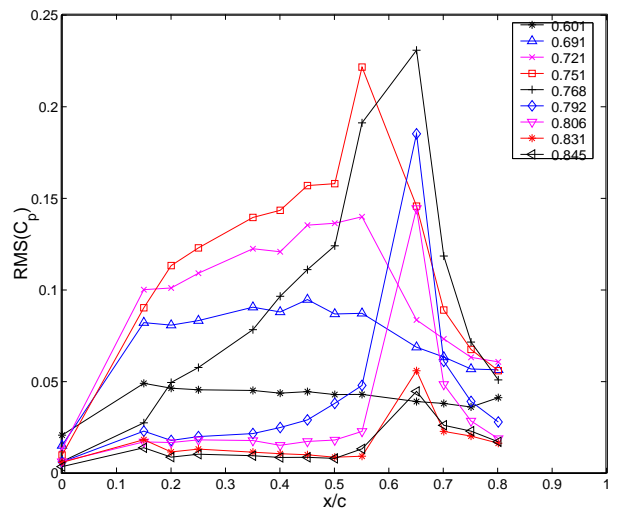


Fig. 9 Fluctuations of the upper surface pressure coefficients for different Mach numbers at a $\bar{\alpha} = 1.5^\circ$ and $\Delta\alpha = 0.2^\circ$

The formation of the shock is represented by the rising levels between the 55% and 65% sensor locations. Slightly higher values can be observed

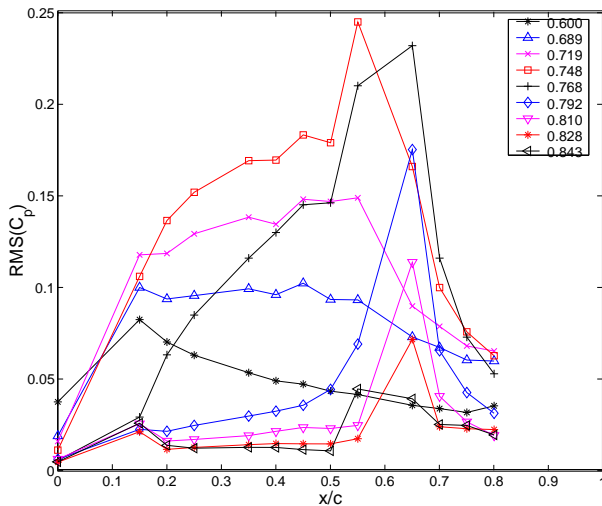


Fig. 10 Fluctuations of the upper surface pressure coefficients for different Mach numbers at a $\bar{\alpha} = 1.5^\circ$ and $\Delta\alpha = 0.4^\circ$

for the higher amplitudes particularly in the forward part of the airfoil. That may partly be an effect of the transition. One result from the steady test series was that the pressure distribution was most sensitive to the transition fixing for an angle of attack of 2° since the local pressure coefficient at the fixing location of 5% then often was near the critical pressure coefficient C_p^* . Another reason may be the formation of a supersonic area in that region as from Mach numbers of 0.72. As a consequence the pitching motion causes that part of the flow to permanently change its situation between sub- and supersonic state.

Furthermore it can be seen that maximum fluctuation levels occur for Mach numbers of 0.75 to 0.77 which is not only the case in the region of the shock but overall on the upper side. Since this is likely due to a higher fluctuation level of the incoming flow, one should be careful with an (over)interpretation at this point.

The interaction between the pitching motion and the airfoil flow can be studied by means of the unsteady pressure distributions. For Mach numbers of 0.77 and 0.84, respectively, and a mean angle of attack of 1.5° , Figures 11 & 13 show the mean and Figures 12 & 14 the corresponding unsteady pressure distributions with respect to the pitching motion. They are determined from a cross spec-

tral analysis of the recorded time signals of the pressure and the pitching motion $\alpha(t)$ in radians. The real part is in phase with the pitch oscillations and the imaginary part is shifted by 90° .

In the first case (Fig. 11, 12) the pressure distribution shows the strongest dependency on the pitching motion for both real and imaginary parts in the upper forward part of the airfoil around 20% to 30% chord. This corresponds to the observations mentioned above concerning the higher fluctuation levels in that region. The second case for the higher Mach number still shows an in-phase relationship in the upper forward airfoil region but an even stronger effect of the pitching motion on the upper and lower airfoil surface pressure distribution in the region of the shocks. Due to a failure of the sensor at 60% chord on the upper side the values at that position are unknown. Nevertheless it can clearly be derived from the signals of both adjacent sensors that the sign of the real part changes which is pointing out a flow separation. This sign change at the location of the shock can be observed as of a Mach number of 0.79 which corresponds with the change in the slope of the steady pitching moment. As a consequence this would indicate a relationship between the extent of the shock-induced separation and the decrease of the damping observed during the free oscillation tests.

4 Summary

This paper gives an survey of the measured steady and unsteady aerodynamic data of a pitching rectangular wing section in two-dimensional transonic flow. The results of steady pressure measurements with a fixed model are presented as background information for a better understanding of the unsteady flow around the supercritical airfoil undergoing free and forced pitch oscillations. During the experiments with decaying, i.e., free oscillations of the elastically mounted wing section no unstable case was found but a trend of the determined damping coefficients could be observed that leads to the assumption of a torsional instability at Mach numbers above 0.85. Potential reasons were sought in the behaviour of

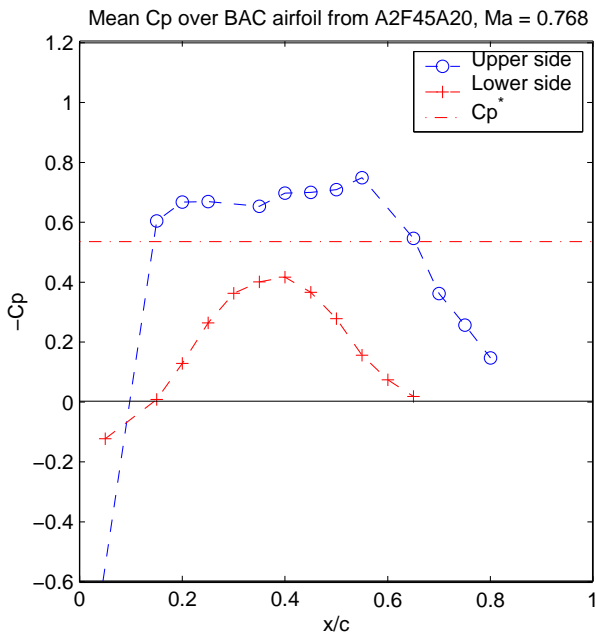


Fig. 11 Mean pressure distribution for Ma = 0.77, $\bar{\alpha} = 1.5^\circ$ and $\Delta\alpha = 0.4^\circ$. $\omega^* = 0.17$.

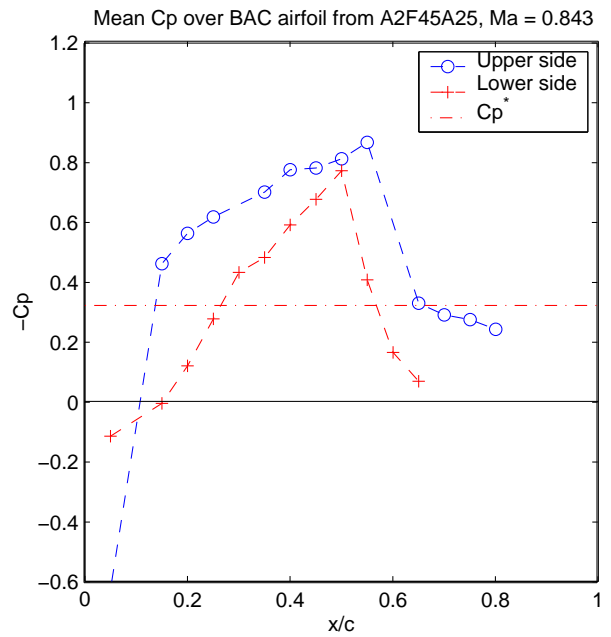


Fig. 13 Mean pressure distribution for Ma = 0.84, $\bar{\alpha} = 1.5^\circ$ and $\Delta\alpha = 0.4^\circ$. $\omega^* = 0.16$.

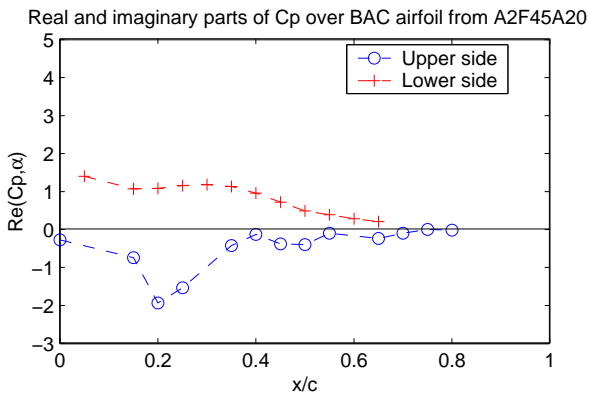


Fig. 12 Unsteady pressure distribution for Ma = 0.77, $\bar{\alpha} = 1.5^\circ$ and $\Delta\alpha = 0.4^\circ$. $\omega^* = 0.17$.

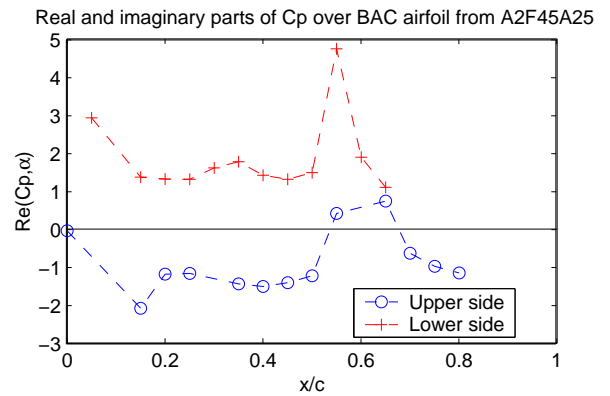
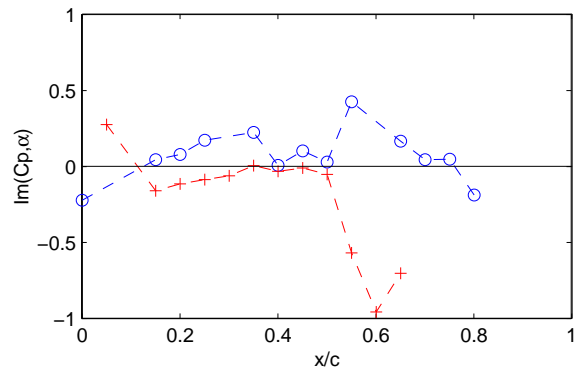
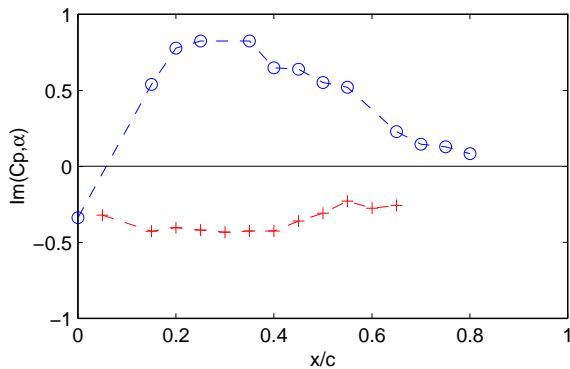


Fig. 14 Unsteady pressure distribution for Ma = 0.84, $\bar{\alpha} = 1.5^\circ$ and $\Delta\alpha = 0.4^\circ$. $\omega^* = 0.16$.



the pitching moment and the lift divergence under steady conditions. The analysis of the forced pitch oscillations concentrated on fluctuations of the airfoil pressure distribution as well as the unsteady pressure coefficients. Some assumptions were made concerning the influence of supersonic areas in the surrounding flow field and of flow separation, again with the aid of steady data.

5 Remarks

The experiments are carried out at the *Aerodynamisches Institut Aachen* within the frame of the collaborative research centre SFB 401 of the *Rheinisch-Westfälische Technische Hochschule Aachen*: “Modulation of Flow and Fluid-Structure Interaction at Airplane Wings” (<http://www.lufmech.rwth-aachen.de/sfb401/>).

We appreciate the straightforward and kind cooperation with the staff of DLR Göttingen, Institut für Aeroelastik [8, 9], who gave us many helpful hints particularly concerning the experimental setup and the general configuration.

Literatur

- [1] Amecke J. Direkte Berechnung von Wandinterferenzen und Wandadaptation bei zweidimensionaler Strömung in Windkanälen mit geschlossenen Wänden. Forschungsbericht, DFVLR-FB 85-62, 1985.
- [2] Drela M. *Two-Dimensional Transonic Aerodynamic Design and Analysis using the Euler Equations*. PhD thesis, Massachusetts Institute of Technology, 1985.
- [3] Hillenherms C, Limberg W, and Schröder W. Experimental Setup for Transonic Flow over a 2-D Rectangular Wing Section Oscillating in Pitch. *Proc Proc. 22nd Congress of the International Council of the Aeronautical Sciences*, Harrogate (UK), 27 Aug. - 1 Sept. 2000. ICAS-2000-3.1.3.
- [4] Hillenherms C, Schröder W, and Limberg W. Unsteady Force and Pressure Measurements on an Oscillating Rectangular Wing Section in Transonic Flow. *Proc Proc. 19th AIAA Applied Aerodynamics Conference*, Anaheim (CA), 11-14 June 2001. AIAA Paper 2001-2468.
- [5] Hufnagel K. *Entwicklung und Optimierung von Sechs-Komponenten-DMS-Windkanalwaagen zum Einsatz unter kryogenen Bedingungen*. Dissertation, TH Darmstadt, 1995.
- [6] Moir I. Measurements on a two-dimensional aerofoil with high-lift devices. AGARD-AR-303, DRA, Farnborough, 1994.
- [7] Romberg H.-J. *Experimentelle Untersuchung der schallnahen Umströmung eines superkritischen Tragflügelprofils unter besonderer Berücksichtigung von Windkanalinterferenzen*. Dissertation, RWTH Aachen, März 1990.
- [8] Schewe G and Deyhle H. Experiments on Transonic Flutter of a Two-Dimensional Supercritical Wing with Emphasis on the Non-Linear Effects. *Proc Proceedings of the Royal Aeronautical Society Conference on “Unsteady Aerodynamics”*, 17-18 July 1996.
- [9] Schewe G, Knipfer A, Mai H, and Dietz G. Experimental and numerical investigation of non-linear effects in transonic flutter. Technical report, DLR IB 232-2002 J 01, 2002.
- [10] Voß R. *AGARDograph 336: Wind Tunnel Wall Corrections*, chapter Wall Correction Methods for Dynamic Tests, pp 9-1 – 9-29. NATO AGARD, 1998.